Bioorganic & Medicinal Chemistry Letters 20 (2010) 571–575

Contents lists available at ScienceDirect

Bioorganic & Medicinal Chemistry Letters

journal homepage: www.elsevier.com/locate/bmcl

Optimization of piperidyl-ureas as inhibitors of soluble epoxide hydrolase

Anne B. Eldrup *, Fariba Soleymanzadeh, Neil A. Farrow, Alison Kukulka, Stéphane De Lombaert

Department of Medicinal Chemistry, Boehringer Ingelheim Pharmaceuticals, Ridgefield, CT 06877, United States

ARTICLE INFO

Article history:
Received 27 October 2009
Revised 16 November 2009
Accepted 17 November 2009
Available online 22 November 2009

Keywords:
sEH
Soluble epoxide hydrolase
EETs
Epoxide eicosatrienoic acids

ABSTRACT

Inhibition of sEH is hypothesized to lead to an increase in epoxyeicosatrienoic acids resulting in the potentiation of their anti-inflammatory and vasodilatory effects. In an effort to explore sEH inhibition as an avenue for the development of vasodilatory and cardio- or renal-protective agents, a lead identified through high-throughput screening was optimized, guided by the determination of a solid state co-structure with sEH. Replacement of potential toxicophores was followed by optimization of cell-based potency and ADME properties to provide a new class of functionally potent sEH inhibitors with attractive in vitro metabolic profiles and high and sustained plasma exposures after oral administration in the rat.

Soluble epoxide hydrolase (sEH) promotes the metabolism of biologically active epoxyeicosatrienoic acids (EETs) to dihydroxy epoxyeicosatrienoic acids (DHETs).[1] In recent reports EETs have been described as anti-inflammatory and vasodilatory mediators, suggesting that the inhibition of sEH might provide an avenue for the development of therapeutics for indications such as hypertension and end-organ protection, through increased EETs levels.[2–4]

Inhibitors of sEH typically include a central urea pharmacophore believed to engage in hydrogen bond formation with active site residues Tyr383, Tyr466 and Asp335.[5–8] Large, hydrophobic domains flank the central urea pharmacophore, resulting in highly hydrophobic molecules with low polar surface areas (Fig. 1).[8–12] Consequently, a number of recent reports have focused on the optimization of physiochemical properties for inhibitors such as AUDA.[13,11]

We recently decided to explore sEH inhibition as an avenue for the development of vasodilatory and cardio- or renal-protective agents. In order to achieve the best possible starting point for lead optimization, we performed a high-throughput screen of our in-house compound collection using an assay that measures the displacement of a rhodamine-labeled probe from human sEH.[14] In this screen, several potent leads were identified, including 1-4-(1*H*-pyrrol-1-yl)-*N*-[4-(trifluoromethoxy)phenyl]-piperidinecarboxamide (**1**, IC_{50} 11 nM) (Fig. 2).[15] Based on its potent inhibition of sEH activity, **1** was selected as the starting point for a lead optimization process.

Our evaluation of the structure–activity relationship (SAR) for **1** initially focused on the replacement of the two potential toxicophores, the pyrrole and the 4-trifluoromethoxyaniline moieties. Compounds for SAR evaluation were prepared by standard synthetic methods, from commercially available starting materials, or from starting materials synthesized by reported methods (Scheme 1). The ability of our SAR compounds to bind sEH by the displacement of a rhodamine-labeled probe from human sEH was assessed as a measure of sEH inhibition.[14,15]

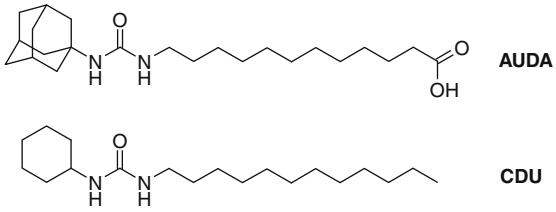

Figure 1. Chemical structure of the sEH inhibitors 12-(3-adamantan-1-yl-ureido)dodecanoic acid (AUDA) and 1-cyclohexyl-3-dodecylurea (CDU).

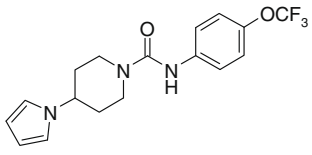

1
hsEH IC_{50} = 11nM

Figure 2. Chemical structure of the sEH inhibitor, 1-4-(1*H*-pyrrol-1-yl)-*N*-[4-(trifluoromethoxy)phenyl]-piperidinecarboxamide (**1**), identified through high-throughput screening.

* Corresponding author.
E-mail address: anne.eldrup@boehringer-ingelheim.com (A.B. Eldrup).

0960-894X/$ - see front matter © 2009 Elsevier Ltd. All rights reserved.
doi:10.1016/j.bmcl.2009.11.091

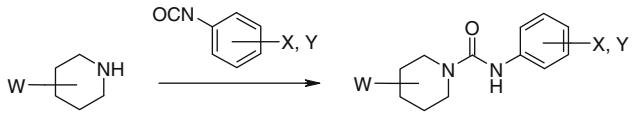

Scheme 1. General synthetic scheme for the preparation of compounds **1** through **47**.

In the first set of compounds, the left-hand side pyrrole was either omitted or replaced with a small, polar moiety such as hydroxymethyl, or with methyl (Table 1, compounds **2**, **3** and **6**). Omission of the pyrrole moiety to give **2** resulted in a small, 2-fold, decrease in the binding affinity for sEH (IC_{50} 24 nM), indicating that the pyrrole moiety is not required for recognition by sEH. Replacement of the pyrrole with hydroxymethyl (IC_{50} 46 nM) or methyl (IC_{50} 18 nM) was tolerated, although not preferred (Table 1, compounds **3** and **6**). The effect of a change in the regiochemistry of the hydroymethyl or methyl substituents was also examined but did not markedly improve the inhibitory potency of these compounds (Table 1, compounds **4**, **5**, **7** and **8**). The effect of the introduction of an acidic or basic moiety was assessed with compounds **9** and **10**, respectively (Table 1). These compounds suffered a substantial loss of inhibitory potency (IC_{50}s >3000 nM).

In another set of compounds, featuring the 3-hydroxymethylpiperidine left-hand side, the 4-trifluoromethoxyaniline right-hand side was replaced with a variety of benzyl amines (Table 2). The replacement of 4-trifluoromethoxyaniline with unsubstituted benzyl amine (Table 2, compound **11**) led to a substantial loss of inhibitory potency (IC_{50} >3000 nM). A beneficial effect of substitution was measurable when a methyl group was placed in the 2- or the 4-position (IC_{50}s 1500 and 2900 nM, for **12** and **14**, respectively), whereas methyl substitution of the benzylic position, or the 3-position, resulted in compounds with no measurable inhibitory potency. In a further effort to identify a preferred, non-aniline, right-hand side, the effect of concomitant substitution of the 2- and 4-positions was investigated by the synthesis of the 2,4-dichloro-substituted analog **16** (Table 2). Profiling of **16** revealed inhibitory potency in range with the original lead compound **1** (IC_{50} 41 nM). The importance of the regiochemistry of the benzyl substitution was confirmed by the evaluation of the corresponding 3,4-dichloro-substituted analog **17**. The potency of this analog (IC_{50} 200 nM) was reduced 5-fold compared to **16** (Table 2). The effect of an extension of the tether to the 2,4-dichlorophenyl moiety was examined by the synthesis of its phenethyl analog **18**, for which inhibitory potency was found to be 5–6-fold reduced compared to **16**. Taken together, these results suggested to us that 2,4-dichlorobenzyl is likely a privileged motif for sEH inhibition, and further SAR exploration was performed in the context of the 2,4-dichlorobenzyl right-hand side. In parallel with further SAR exploration, an effort to identify possible alternatives to the 2,4-dichlorobenzyl moiety was undertaken by our high throughput chemistry group. This work will be published elsewhere.

Having identified replacements for both the pyrrole and 4-trifluoromethoxyaniline moieties, we returned our attention to the SAR of the left-hand side piperidine with the goal to improve the inhibitory potency against sEH compared to the original lead compound **1**.

The effect of substitution of the left-hand side piperidine was now explored by the synthesis of a set of compounds derived from the isonipecotic acid derivative **19** (Table 3). In the context of the 2,4-dichlorobenzyl based right-hand side, the introduction of the negatively charged carboxy substituent in the piperidine 4-position piperidyl resulted in a 40-fold loss in inhibitory potency (Table 3, compound **19**, IC_{50} 1000 nM), whereas for compound **9**, a substantial loss of inhibitory potency had been observed. Structural modification to the corresponding amide resulted in a 4-fold improvement in inhibitory potency for sEH (Table 3, compound **20**, IC_{50} 220 nM). Nonetheless, further elaboration from this starting point to include larger, polar substituents such as tethered pyrans, pyrrolidines, methylsulfonyl, or methoxy did not result in improvements in inhibitory potency (Table 3, compounds **21** through **25**, IC_{50}s ranging from 150 to 230 nM), suggestive perhaps of limited interaction between the left-hand side tethered moieties and the enzyme.

The SAR of the left-hand side piperidine was further explored by the synthesis of a number of analogs with directly linked or tethered aromatic left-hand sides (Table 4, compounds **26** through **35**). Our profiling of these compounds revealed much improved inhibitory potencies compared to the compounds with the tethered heteroalkyl left-hand sides (IC_{50}s ranging from 4.3 to 39 nM). Most compounds with directly attached aryl substituents and certain compounds with oxy-tethered aryl substituents displayed inhibitory potencies in the low nanomolar range (Table 4, IC_{50}s of 6.0, 5.6, and 4.3 nM for compounds **26**, **28**, and **32**,

Table 1
Inhibitory potencies (IC_{50}s) of analogs of the lead compound **1**

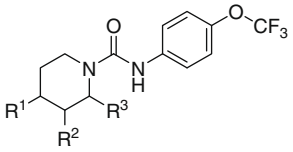

Compd	R^1	R^2	R^3	sEH IC_{50} (nM)
1	2-Pyrrolyl	H	H	11
2	H	H	H	24
3	$HOCH_2$	H	H	46
4	H	$HOCH_2$	H	19
5	H	H	$HOCH_2$	110
6	CH_3	H	H	18
7	H	CH_3	H	12
8	H	H	CH_3	29
9	HOOC	H	H	>3000
10	*N*-Piperidinyl	H	H	>3000

In these compounds, the left-hand side pyrrole was either omitted or replaced with hydroxymethyl, with methyl, or with an acidic or basic moiety. The effect of a change in the regiochemistry of the piperidine substituent was also examined.

Table 2
Inhibitory potencies (IC_{50}s) of analogs of compound **4**

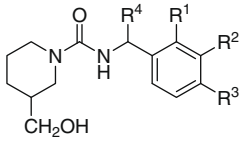

Compd	R^1	R^2	R^3	R^4	sEH IC_{50} (nM)
11	H	H	H	H	>3000
12	CH_3	H	H	H	1500
13	H	CH_3	H	H	>3000
14	H	H	CH_3	H	2900
15a,15b[a]	H	H	H	CH_3	>3000
16	Cl	H	Cl	H	41
17	H	Cl	Cl	H	200
18[b]	Cl	H	Cl	H	230

In these compounds, the right-hand side 4-trifluoromethoxyaniline was replaced with methyl- or chloro-substituted benzylamines.

[a] Enantiopure benzylamines were utilized in the synthesis of **15a** and **15b** resulting in diastereoisomeric mixtures of *R*,*S*-3-hydroxymethylpiperidinyl derived ureas. The diastereoisomeric mixtures containing either *R*- or *S*-α-methylbenzylamine were profiled separately.

[b] Compound **18** incorporates an ethylene linker to the 2,4-dichlorophenyl moiety.

Table 3
Inhibitory potencies (IC_{50}s) of analogs of compound **16**

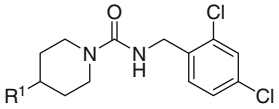

Compd	R^1	sEH IC_{50} (nM)
19	COOH	1000
20	CONH2	220
21	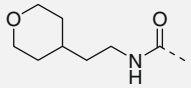	150
22	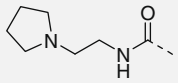	220
23	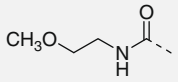	210
24	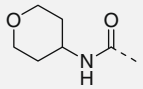	180
25	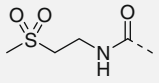	230

In these compounds analogs based on isonipecotic acid were examined the context of a 2,4-dichlorobenzyl-based right-hand side.

respectively), whereas analogs in which the aryl group was tethered through carbon, nitrogen, or through a sulfonyl or sulfonamide moiety appeared slightly less potent inhibitors of sEH (Table 4, IC_{50}s of 12, 15, 35, 39, and 17 nM for compounds **29**, **30**, **31**, **34**, and **35**, respectively).

To better understand if the aryl-oxy class of sEH inhibitors was an appropriate starting point for further optimization, compound **32** and its less potent but more soluble analog **33** were evaluated for their inhibitory potencies in a cell-based assay,[15] their selectivity against the EETs-generating CYP 2J2, CYP 2C9, and CYP 2C19 isoforms, as well as their in vitro stability in human and rat liver microsomes and their exposure in rat plasma after oral dosing (Fig. 3).

Profiling of **32** and **33** revealed similar cell-based potencies. The phenoxy derivative **32** was less selective against EETs-generating CYP isoforms compared to the pyrimidine-oxy derivative **33**, and displayed sub-optimal stability in both human and rat liver microsomes ($t_{1/2}$ 7 and 21 min, respectively). In contrast, the in vitro

Table 4
Inhibitory potencies (IC_{50}s).of analogs of compound **16**

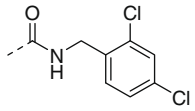

Compd	R^1	sEH IC_{50} (nM)
26	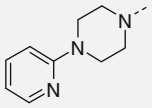	6.0
27	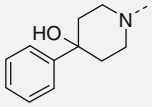	27
28	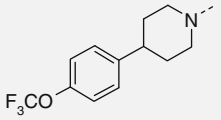	5.6
29	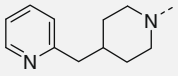	12
30	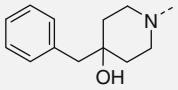	15
31	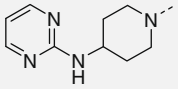	35
32	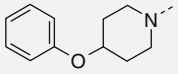	4.3
33	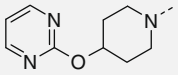	15
34	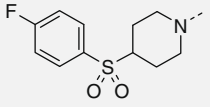	39
35	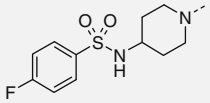	17

In these compounds, the effect of an introduction of a directly linked or one-atom tethered aromatic left-hand side was evaluated.

metabolic stability of compound **33** was greater ($t_{1/2}$ 86 and 37 min, in human and rat liver microsomes, respectively) suggest-

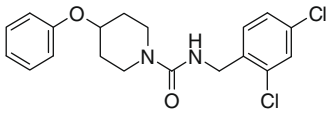

32

human sEH IC_{50} = 4.3 nM
ELISA IC_{50} = 5.1 nM
2J2/2C9/2C19 IC_{50}= 1.4 / 1.4 / ND μM
$t_{1/2}$ in hLM = 21 min
$t_{1/2}$ in rLM = 7 min
Solubility = 3.4 μg/mL
Exposure (5 mpk PO; 4h) = 0.1 μM

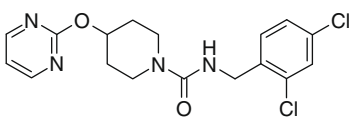

33

human sEH IC_{50} = 15 nM
ELISA IC_{50} = 15 nM
2J2/2C9/2C19 IC_{50}= 20 / 20 / 19 μM
$t_{1/2}$ in hLM = 86 min
$t_{1/2}$ in rLM = 37 min
Solubility = 174 μg/mL
Exposure (5 mpk PO; 4h) = 1.3 μM

Figure 3. Results from profiling of compounds **32** and **33** for cell-based potency, selectivity against CYP 2J2, CYP 2C9 and CYP 2C19, in vitro stability in liver microsomes and exposure in rat after per oral dosing.

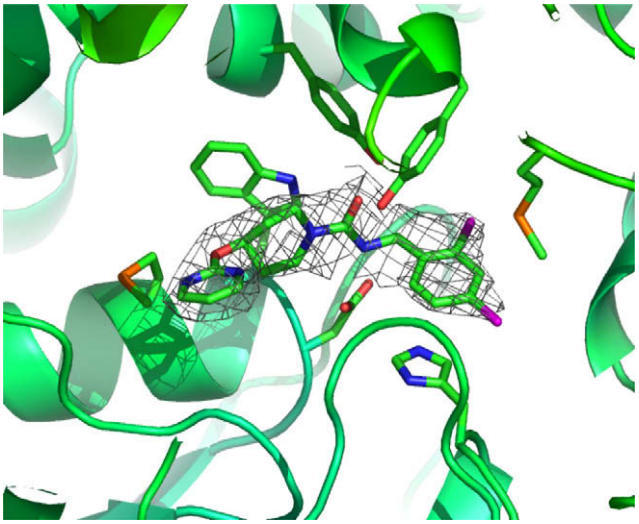

Figure 4. The solid state structure of the co-complex of **33** and human sEH shows the chloro groups of the 2,4-dichlorobenzyl amine moiety pointing towards right hand side pockets in the enzyme. The pocket occupied by the 2-chloro moiety is buried in the protein providing only limited opportunities for optimization. In contrast, the left hand side pyrimidine is exposed to solvent. Coordinates of the co-structure with compound **33** deposited as 3KOO with the RCSB protein data bank.

ing that functionalization to increase the polar surface area (PSA) could be a path to prevent the observed rapid in vitro metabolism of **32**. In line with these observations, **32** did not display sustained plasma exposure after oral administration to rat, while **33** maintained micromolar plasma levels at 4 h post dosing, hence implying the existence of an in vitro/in vivo correlation.

The co-crystal structure of **33** (which displays increased solubility compared to **32**) and sEH was determined to guide the design of compounds with improved ADME properties. Close examination of the solid state structure revealed the amide moiety of **33** positioned with the carbonyl oxygen directed towards the active site Tyr383 and Tyr466 and the urea proton directed towards the Asp335 residue (Fig. 4). In this structure, the chloro substituents of the 2,4-dichlorobenzyl amine are positioned pointing towards two separate hydrophobic regions of the enzyme, with the pocket occupied by the 2-chloro substituent buried in the protein. In contrast, the left hand side pyrimidine is exposed to solvent.

Based on our examination of the solid state structure of **33**, further optimization was carried out with the goal to improve ADME properties. Our examination of the co-crystal structure of **33** had revealed that the left-hand side aromatic moiety was exposed to solvent, and we hypothesized that substitution to improve ADME properties would likely be possible without negatively impacting potency. Hence, the effect of fluoro, chloro, trifluoromethoxy, cyano, methylsulfonyl, methylamido, methylsulfonamido, and carboxy substitution of the 4-position on the aryl-oxy left-hand side phenoxy moiety of **32** was examined (Table 5, compounds **36** through **38**, **41**, and **44** through **47**). The inhibitory potencies of these compounds were largely unchanged compared to **32** (IC_{50}s ranging from 4.2 to 12 nM). A transposition of the cyano or sulfonamide substituents to the 2- or 3-position also did not result in marked changes in inhibitory potency (Table 5, compound, **39**, **40**, **42** and **43**, IC_{50}s of 3.9, 4.9, 4.9 and 4.6 nM). However, evaluation of compounds **36**–**47** in our cell-based assay, revealed relatively large differences in potencies (Table 5, EC_{50}s ranging from 0.25 to 18 nM), suggesting that the binding assay does not accurately reflect the potency for compounds with IC_{50}s less than 4–5 nM. This limitation is consistent with the measured K_d of the probe (4.3 nM)[14] and the enzyme concentration used in the binding assay (10 nM).[15]

Table 5
Inhibitory potencies (IC_{50}s) of analogs of compound **32**

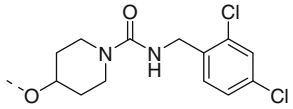

Compd	R^1	sEH IC_{50} (nM)	ELISA EC_{50} (nM)	$t_{1/2}$ hLM/rLM (min)
36	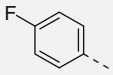	6.1	4.2	34/20
37	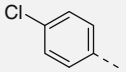	5.9	10	77/24
38	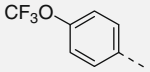	12	18	86/77
39	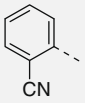	3.9	0.44	8.0/6.0
40	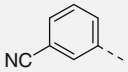	4.9	0.63	47/13
41	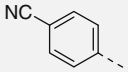	4.2	0.78	35/12
42	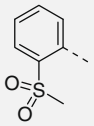	4.9	1.65	4.0/4.0
43	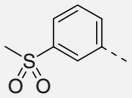	4.6	0.25	20/9.0
44	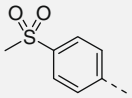	5.6	0.97	27/46
45	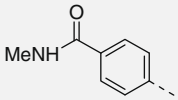	4.2	0.34	17/11
46	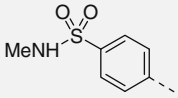	5.2	0.29	12/40
47	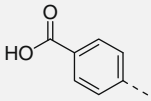	6.4	1.7	273/172

In these compounds, the left-hand side piperidine substitution was optimized for intrinsic and cell-based inhibitory potencies. The in vitro metabolic stabilities of these compounds in both human and rat liver microsomes were also evaluated.

Our results from the cell-based assay indicated that compounds with polar substituents such as cyano, sulfonylmethyl, methylamido, or methylsulfonylamido were more potent inhibitors of sEH activity in cells, compared to compounds with halogen or trifluoromethyl substituents (Table 5, compounds **36** through **47**). Evaluation of the in vitro metabolic stability profiles for compounds **36**–**47** revealed poor metabolic stability profiles for compounds with 2-substitution (Table 5, compounds **39** and **42**) and for compounds with methylamido and methylsulfonamido substituents (Table 5, **45** and **46**). Most other analogs displayed intermediate in vitro stabilities (Table 5, compounds **36**–**38**, **40**, **41**, and **43**–**46**), with the exception of the carboxylic acid derivative **47**, which demonstrated excellent in vitro metabolic stability in both human and rat liver microsomes.

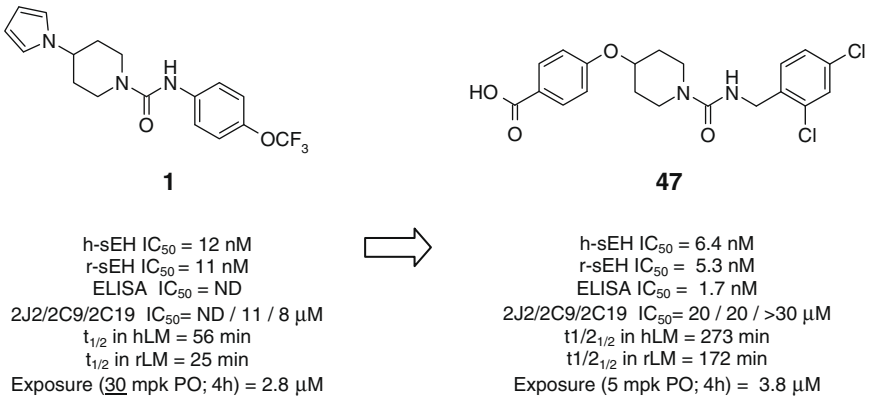

Figure 5. Chemical structures and profiles for compound **47** compared to that of the lead compound **1**. Potential toxicophores were replaced. Improvements in CYP 450 selectivity, in vitro stability, and in vivo plasma exposure after per oral dosing, were achieved.

Based on its potency in cells and its excellent in vitro stability in microsomes, the profiling of compound **47** was extended to include its ability to inhibit CYP 2J2, 2C9, and 2C19, and its pharmacokinetic profile in rat was evaluated (Fig. 5). Compound **47** was found to be highly selective against these EETs-forming CYP 450 isoforms (IC_{50}s 20 μM or greater) and determination of its plasma exposure following oral dosing in the rat, revealed high and sustained exposures (1.70, 2.66, 3.83 and 5.43 μM at the 1, 2, 4, and 6 h time points, respectively).

In summary, the lead compound **1**, identified through high-throughput screening, was optimized to provide a class of novel, potent, and orally bioavailable sEH inhibitors.[16] In addition to the replacement of potential toxicophores and optimization of cell-based potencies, improvements of in vitro and in vivo ADME properties were achieved leading to the identification of a class of sEH inhibitors, exemplified by **47**, a potent sEH inhibitor with an attractive metabolic stability profile in rat and human liver microsomes and high and sustained plasma exposure in the rat after oral administration.

During the preparation of this manuscript, publications appeared that describe the properties of a class of sEH inhibitors that incorporate a regioisomeric piperidine motif.[17–19]

Acknowledgments

We thank Dr. Michael August and Ms. Lori Patnaude for performing the high-throughput screen of our compound collection against sEH.

References and notes

1. Spector, A. A.; Fang, X.; Snyder, G. D.; Weintraub, N. L. *Prog. Lipid Res.* **2004**, *43*, 55.
2. Imig, J. D.; Zhao, X.; Capdevila, J. H.; Morisseau, C.; Hammock, B. D. *Hypertension* **2002**, *39*, 690.
3. Imig, J. D. *Am. J. Physiol.* **2005**, *289*, 496.
4. Batchu, S. N.; Law, E.; Falck, J. R.; Seubert, J. M. *J. Mol. Cell. Cardiol.* **2009**, *46*, 67.
5. Gomez, G. A.; Morisseau, C.; Hammock, B. D.; Christianson, D. W. *Biochemistry* **2004**, *43*, 4716.
6. Argiriadi, M. A.; Morisseau, C.; Hammock, B. D.; Christianson, D. W. *Proc. Natl. Acad. Sci. U.S.A.* **1999**, *96*, 10637.
7. Gomez, G. A.; Morisseau, C.; Hammock, B. D.; Christianson, D. W. *Protein Sci.* **2006**, *15*, 58.
8. Argiriadi, M. A.; Morisseau, C.; Goodrow, M. H.; Dowdy, D. L.; Hammock, B. D.; Christianson, D. W. *J. Biol. Chem.* **2000**, *275*, 15265.
9. Morisseau, C.; Goodrow, M. H.; Dowdy, D.; Zheng, J.; Greene, J. F.; Sanborn, J. R.; Hammock, B. D. *Proc. Natl. Acad. Sci. U.S.A.* **1999**, *96*, 8849.
10. Kim, I.-H.; Morisseau, C.; Watanabe, T.; Hammock, B. D. *J. Med. Chem.* **2004**, *47*, 2110.
11. Kim, I.-H.; Heirtzler, F. R.; Morisseau, C.; Nishi, K.; Tsai, H.-J.; Hammock, B. D. *J. Med. Chem.* **2005**, *48*, 3621.
12. Kim, I.-H.; Tsai, H.-J.; Nishi, K.; Kasagami, T.; Morisseau, C.; Hammock, B. D. *J. Med. Chem.* **2007**, *50*, 5217.
13. Kim, I.-H.; Morisseau, C.; Watanabe, T.; Hammock, B. D. *J. Med. Chem.* **2004**, *47*, 2110.
14. The high-throughput screen used a rhodamine-labeled probe with a K_d of 4.3 nM. The synthesis and characterization of the probe is described in detail in: Ingraham, R. H.; Cardozo, M. G.; Grygon, C. Anne; Kroe, R. Rebecca; Proudfoot, J. R. WO 02/082082.
15. Eldrup, A. B.; Soleymanzadeh, F.; Taylor, S. J.; Muegge, I.; Farrow, N. A.; Joseph, D.; McKellop, K.; Man, C. C.; Kukulka, A.; De Lombaert, S. *J. Med. Chem.* **2009**, *52*, 5880.
16. Delombaert, S.; Eldrup, A. B.; Kowalski, J. A.; Mugge, I. A.; Soleymanzadeh, F.; Swinamer, A. D.; Taylor, S. J. WO 07/106705.
17. Shen, H. C.; Ding, F.-X.; Wang, S.; Xu, S.; Chen, H.; Tong, X.; Tong, V.; Mitra, K.; Kumar, S.; Zhang, X.; Chen, Y.; Zhou, G.; Pai, L.-Y.; Alonso-Galicia, M.; Chen, X.; Zhang, B.; Tata, J. R.; Berger, J. P.; Colletti, S. L. *Bioorg. Med. Chem. Lett.* **2009**, *19*, 3398.
18. Colletti, S. L.; Shen, H.; Ding, F.-X. WO 09/011872.
19. Shen, H. C.; Ding, F.-X.; Wang, S.; Deng, Q.; Zhang, X.; Chen, Y.; Zhou, G.; Xu, S.; Chen, H.; Tong, X.; Tong, V.; Mitra, K.; Kumar, S.; Tsai, C.; Stevenson, A. S.; Pai, L.-Y.; Alonso-Galicia, M.; Chen, X.; Soisson, S. M.; Roy, S. E.; Zhang, B.; Tata, J. R.; Berger, J. P.; Colletti, S. L. *J. Med. Chem.* **2009**, *52*, 5009.